MICROSTRUCTURE CONTROL OF SUPER-HIGH STRENGTH ALUMINIUM ALLOYS

Kozo OSAMURA*, Hiroki ADACHI*, Hiroshi OKUDA*, Shojiro OCHIAI, Jun KUSUI*** and Kazuhiko YOKOE*****

* Department of Materials Science and Engineering,
Kyoto University, Kyoto 606-0024, Japan
** Mesoscopic Materials Research Center,
Kyoto University, Kyoto 606-0024, Japan
*** Research and Development Laboratory, Toyo Aluminium K.K.,
Shiga 529-16, Japan

ABSTRACT Super-high strength aluminium alloys (Mesoalite) have been recently developed. In order to achieve further improvement, the Zn/Mg composition ratio of the alloys was changed. The effective ratio dependence of Guinier radius, interparticle distance and volume fraction of precipitates was well explained by a hypothetical phase diagram with two metastable phases. During isothermal aging at 383 K, all the alloys with different Zn/Mg ratio showed a maximum Vickers hardness nearly for 108 ks, where very high hardness was observed for the alloys containing T′ metastable phase. The highest Vickers hardness was 269 (converted yield stress of 1120 MPa) resulting to the largest coherency strain around precipitates.

Keywords: super-high strength, aluminium alloy, metastable phase, coherency strain, Vickers hardness

1. INTRODUCTION

Industrial aluminium alloys are classified into eight families depending on their alloy composition, where some of them are so called heat-treatment alloys showing high strength. Their high strength is mainly attributed to metastable phases, for instance, the 7000 series alloys are well known to be strengthened by η' metastable phase. Beside those commercial alloys, a series of super-high strength aluminium

alloys (Mesoalite) have been recently developed by means of powder metallurgy[1], of which the standard properties are σ_{UTS} = 990 MPa and $\Delta L/L$ = 0.8% with a typical composition of Al-9.5Zn-3Mg-1.5Cu-4Mn-0.04Ag-0.5Zr in wt% [2] .In order to clarify the structural chracteristics and achieve further improvements, the optimization of microstructure has been attempted in the present study.

2. EXPERIMENTAL PROCEDURE

The chemical composition of the alloys used here is summarized in Table 1. In order to investigate an effect of solute concentrations on the precipitation behavior, the amounts of Zn and Mg were systematically changed. The powder prepared by air-atomizing was pressed into a rod-like shape by cold isostatic pressing. The rod was first preheated in an argon atmosphere at 773 K for 3.6 ks and then extruded at 773 K to an extrusion ratio of 10. The specimen was solution treated at 763 K for 7.2 ks, then water quenched and isothermally aged at 383 K for various times. The Vickers hardness measurement was carried out at room temperature. The synchrotron-radiation small angle scattering (SR-SAS) measurements were performed at the Research Institute for High Energy Physics. The Guinier radius, Porod radius, mean radius, interparticle distance and the volume fraction of precipitates were assessed. The microstructure and thermal change were investigated by means of transmission electron microscope and DSC, respectively.

3. EXPERIMENTAL RESULTS

Figure 1 shows a TEM photograph for the specimen #9 aged at 383 K for 108 ks. The metastable precipitates are observed in the matrix. The chemical composition at the local area was analysed by means of AP-FIM techniques[3]. Zn, Mg and Ag are enriched in the metastable precipitates, but no Mn in the matrix and in the

Table 1 Chemical composition in at% of the specimen examined here.

Sample name	#20	#12	#9	#7*	#5	#3	#2
Zn	5.55	5.56	4.7	3.91	3.56	3.07	2.44
Mg	1.9	3.12	3.48	3.52	3.87	4.49	4.39
Cu	0.68	0.72	0.82	0.7	0.67	0.66	0.65
Mn	2.04	2.18	2.1	2	2.07	1.91	1.89
Zr	0.17	0.17	0.17	0.15	0.16	0.16	0.15
Ag	0.012	0.011	0.01	0.15	0.09	0.09	0.011
Fe	0.043	0.07	0.021	0.011	0.026	0.047	0.057
Si	0.032	0.043	0.063	0.026	0.03	0.05	0.07
Al	90.53	88.13	88.64	89.48	89.61	89.61	90.36
[Zn]	4.41	4.21	3.32	2.67	2.21	1.77	1.06
[Mg]	2.14	3.45	3.83	4.06	4.49	5.14	5.02
[Cu]	0.46	0.47	0.59	0.5	0.46	0.46	0.45
Zn/Mg	2.06	1.22	0.87	0.66	0.49	0.34	0.21

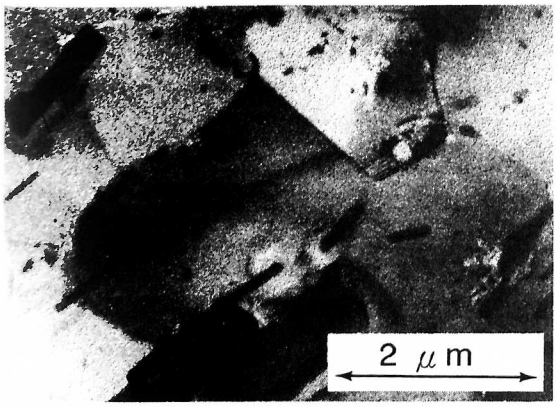

Fig.1 Microstructure of the aged specimen at 383 K for 108 ks.

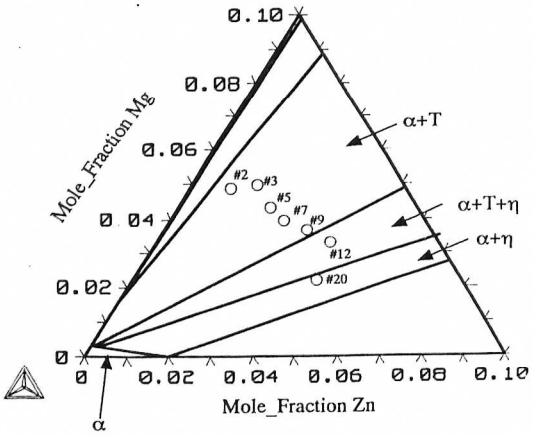

Fig.2 The matrix composition of the specimens.

metastable phase. The chemical composition of rod-like quaternary intermediate phase was Al-15at%Mn- 12at%Zn - 2at%Cu. Ignoring a small amount of copper, a phase field at room temperature was assessed in the relevant Al-Zn-Mg ternary area by means of Thermo-Calc as shown in Fig. 2. By the full formation of Mn quaternary compound, the amount of Zn and Cu is reduced. The location of the matrix composition of each specimen is displayed in the figure.

Fig. 3 shows the aging time dependence of Vickers hardness at 383 K for various specimens with different effective Zn/Mg ratio. The hardness increased with aging time and reached maximum for about 108 ks, then decreased. According to DSC result for the as-quenched specimen #5, a broad endothermal peak was observed at 375 K, which is assigned to the resolution of GP zones. Two exothermic peaks appeared at 445 and 473 K are attributable to the precipitation of T' and T, respectively, because the specimen locates in the α + T two phase field. For the specimen aged at 383 K for 108 ks, an endothermal peak appeared at 440 K is assigned to the resolution of T' phase. Figure 4 shows the change of maximum hardness as a function of effective Zn/Mg ratio. In the α + T two phase field, the hardness increased with increasing the ratio and reached a maximum at the ratio of 0.5. The SR-SAS result provides the structural information about fine metastable precipitates. For the aged specimens with different Zn/Mg ratio, Guinier radius distributes in the range between 2 and 3 nm . The interparticle distance distributes in the range between 9 and 13 nm. Here two type of metastable phases, T' and η' are assumed to appear depending on the relevant equilibrium phase field as shown in Fig. 2. The finer and denser T' precipitates are grown comparing with the η' metastable phase for the same aging condition of 383 K and 108 ks. The volume fraction of precipates is defined as follows;

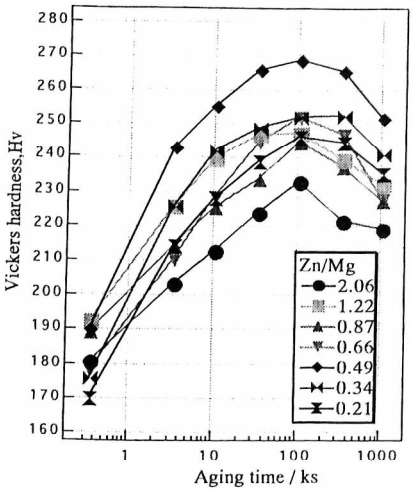

Fig.3 Vickers hardness vs aging time at 383 K.

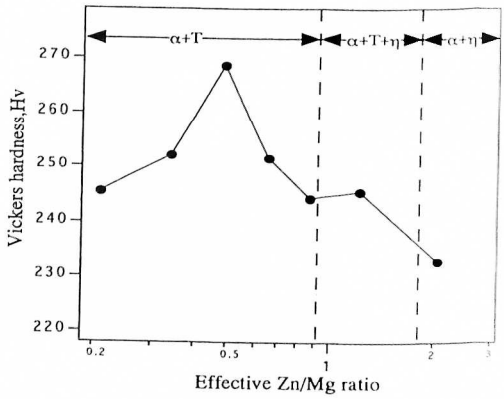

Fig.4 Maximum hardness vs effective Zn/Mg ratio for aged specimens at 383 K.

$$V_f = (4\sqrt{2}\,\pi/3)\,(\mu/l_p)^3 \quad (1)$$

which μ is the mean radius and the l_p is the interparticle distance of metastable precipitates. The effective Zn/Mg ratio dependence is shown in Fig. 5. The volume fraction increased with increasing the effective Zn/Mg ratio and became constant, but it was small for the specimen with the ratio of 2.

The mechanical property is affected by three chracteristic microstructures as shown in Fig. 1. The following summation is suggested [4] for yield stress,

$$\sigma_{obs} = \sigma_{ppt} + \sigma_{fibre} + \sigma_{grain} \quad (2)$$

where σ_{ppt} is the contribution from precipitation hardening, σ_{fibre} is the fibre reinforcement due to the Mn compound and σ_{grain} is the contribution from the grain refinement. The amount of Mn quaternary compound formed during hot extrusion is almost the same for all the specimens examined here, because of the mostly identical Mn concentration as listed in Table 1. During the isothermal aging, the grain growth is supposed not to take place remarkably. Therefore the hardness change shown in Fig. 3 is mainly attributed to the precipitation behavior of metastable phases. As well known, the Vickers hardness is directly connected to the yield stress of the materials. In the previous work, the following empiricalrelation was used[5], $\sigma_y = 0.0163Hv^2 - 0.353Hv + 35.5$. Using this relation, the observed Vickers hardness was converted to the yield stress in the present study. The equivalent yield stress is plotted against $(\mu V_f)^{1/2}$ as shown in Fig. 6. The converted yield stress becomes 1120 MPa for the present highest Vickers hardness of 269. The linear relationship can be observed between two quantities. According to Gerold and Harberkorn's

coherency strain model [6], the yield stress is expressed by the equation,

$$\sigma_y = 3MG|\varepsilon|^{3/2}(\mu V_f/b)^{1/2} \quad (3)$$

where M is the Taylor factor, G is the shear modulus, ε is the coherency strain, and b is the Burgers vector. Comparing the theory of Eq.(3), the coherency strain could be estimated as shown in Fig. 7. Generally the coherency strain is large for T' metastable precipitates, and decreased with increasing the effective Zn/Mg ratio.

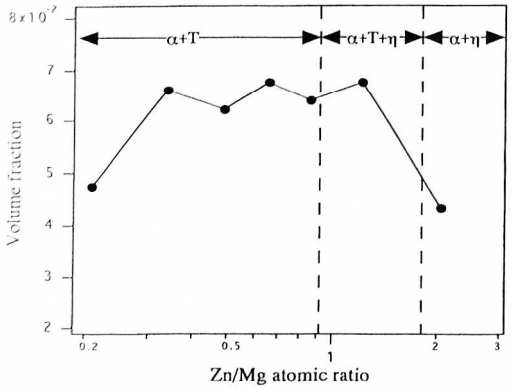

Fig.5 Volume fraction vs effective Zn/Mg ratio for aged specimens at 383 K for 108 ks.

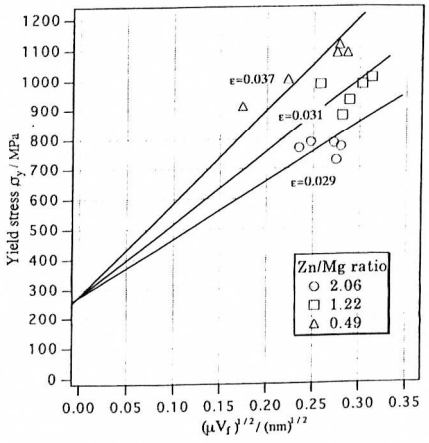

Fig.6 Change of yield stress as a function of $(\mu V_f)^{1/2}$

4. DISCUSSION

Any definite chemical comopsition of η' and T' metastable phases has been not yet reported. So the areas for those two metastable phases are assumed to be present in the relevant equilibrium phase field as shown in Fig. 1. Based on this hypothetical diagram, the present experimental results is discussed as follows.

As shown in Fig. 5, the volume fraction of T' metastable precipitates is larger than that of η' phase. The volume fraction is assessed from the lever rule for the composition difference between the precipitates and the matrix. The experimental result can be clarified from the location of both metastable phases.

The coherency strain tends to increase with increasing Mg concentration as shown experimentally in Fig. 7. The coherency strain is defined as the difference of average atomic size between the precipitate and the matrix. The atomic mismatch between Mg and Al is 11.7%, while it is -1.9 %for Zn atom. Therefore it is suggested that the coherency strain becomes larger for the T' precipitates including richer Mg concentration. The hardness is described as a function of coherency strain, mean radius and volume fraction of precipitates as given by Eq.(3). Owing to the

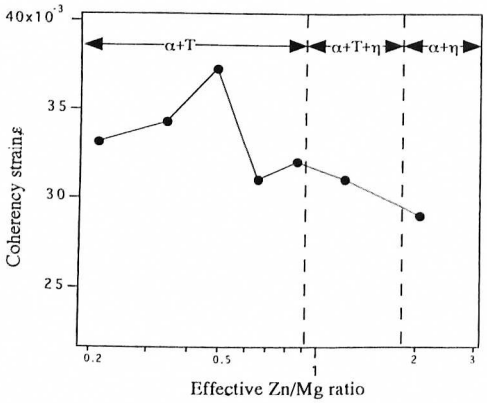

Fig.7 Coherency strain vs effective Zn/Mg ratio for aged specimens at 383 K for 108 ks.

coherency strain and volume fraction as discussed just above, the hardness might become highest for the Mg rich T' metastable phase.

In the present study, many experimental results can be reasonably explained by assuming the existence of two different metastable phases.

5. CONCLUSION

In the present study, the characteristics of their microstructure have been investigated by means of SR-SAS, and TEM techniques as well as the mechanical test. The chemical composition of the matrix locates essentially in the α + T two phase field in the Al-Zn-Mg ternary system. The metastable precipitates in Mesoalite are concluded to be T' phase. The optimum chemical composition to get the highest Vickers hardness was Al-8.0%Zn-3.2%Mg-1.5%Cu-3.9wt%Mn-0.03%Ag in wt%, where the coherency strain and the volume fraction become maximum. The super-high strength realized in the present Mesoalite attributes to the multiple effect of precipitation hardening, fibre reinforcement and fine grain strengthening.

REFERENCES

1. K.Osamura, O.Kubota, P.Promstit, H.Okuda, S.Ochiai, K.Fujii, J.Kusui, T.Yokote and K.Kubo, Metall. and Mater. Tans. A, 26(1995), 1597.
2. J.Kusui, K.Fujii, K.Yokoe, T.Yokote, K.Osamura, O.Kubota and H.Okuda; Mater. Sci.Forum, 217/222(1996), 1823.
3. J.Kusui, K.Yokoe, T.Yokote, K.Osamura, O.Kubota, H.Okuda, K.Hono and T.Sakurai; Proc. Field Emission Symposium (Tsukuba, 1997), in print.
4. K.Osamura, K.Kohno, H.Okuda, S.Ochiai, J.Kusui, K.Fujii, K.Kokoe, T.Yokote and K.Hono; Mater. Sci. Forum, 217/222(1996), 1829.
5. H.Adachi; Thesis for Degree of Master, Graduate School of Kyoto University (1998).
6. V.Gerold and H.Harberkorn; Phys. Stat. Sol., 16(1966), 675.